scientific reports

Check for updates

OPEN

Characterization of RNA editing gene APOBEC3C as a candidate tumor suppressor in prostate cancer

Li-Yang Wang[1,5], Ji Shi[2,5], Mo-Fei Wang[1], Yi-Meng Liu[2], Hong-Shan Guo[2], Jin-Cheng Wang[2], Shu Jiang[2], Jia-Qian Liang[3]✉, Xing-Hua Liao[2]✉ & Shao-Yong Chen[2,4]✉

The human genome encodes 19 adenosine and cytidine deaminase genes, classified as A-to-I versus C-to-U editors. A-to-I editors have been widely identified as a promising therapeutic target in various cancers. Conversely, the investigation into C-to-U editors is relatively limited. This study evaluated RNA-editing genes in prostate cancer (PCa). Notably, the APOBEC3 genes are clustered in terms of their chromosomal locations, and their transcriptional changes exhibit significant positive correlations in both primary PCa and castration-resistant prostate cancer (CRPC). One member of this family, APOBEC3C, is demonstrated here as an androgen receptor (AR)-repressed gene. Consistently, APOBEC3 loci are epigenetically inhibited in PCa progression, with APOBEC3C level lower in PSA-high patients. APOBEC3C-low PCa cohorts exhibit increased resistance to Abiraterone and Enzalutamide. Clinicopathological profiling further confirmed APOBEC3C downregulation along PCa progression to advanced phases (grade IV/V, stage III-IV, and pathological stage T3-4), underscoring its prognostic value. Additionally, APOBEC3C expression inversely correlates with PCa relapse and mortality, and low APOBEC3C levels are linked to unfavorable survival. Notably, integrated analyses identified APOBEC3C as the sole RNA-editing gene with significance in both differential expression and PCa prognosis, and APOBEC3C had the best diagnostic performance among 19 genes. Our efforts provide a foundation for further RNA editors research in PCa diagnosis and therapy, and grant APOBEC3C as a candidate tumor suppressor.

Keywords Prostate cancer, CRPC, RNA-editing, APOBEC3C, Androgen receptor

Prostate cancer (PCa) is a prevalent and highly impactful disease worldwide and a major contributor to cancer-related deaths. The growth and proliferation of PCa cells heavily depend on the androgen receptor (AR) pathway, which drives the transcription of essential cellular programs like central metabolism[1]. The first-line management for PCa is androgen blockade based on castration and AR antagonists. However, despite significant advancements in the diagnosis and treatment of primary PCa, including improved imaging techniques, surgical methods, and targeted therapies, a substantial proportion of patients experience disease progression[2]. Over the course of disease progression, PCa commonly acquires resistance to standard anti-androgen therapies, such as androgen deprivation therapy (ADT), through a range of molecular mechanisms. These include mutations in the androgen receptor (AR)[3], the expression of constitutively active AR splice variants (e.g., AR-V7)[4], and the activation of alternative oncogenic signaling pathways that circumvent AR dependence, such as the PI3K/AKT/mTOR and Wnt/β-catenin pathways[5]. This adaptive resistance frequently results in disease recurrence in a more aggressive and therapy-resistant form, termed castration-resistant prostate cancer (CRPC). CRPC is characterized by persistent tumor proliferation despite castrate levels of circulating androgens, and it is associated with a poor prognosis, metastatic dissemination, and limited therapeutic efficacy[6]. There is a pressing need to identify new

[1]Laboratory of Cell Biology, Genetics and Developmental Biology, Shaanxi Normal University College of Life Sciences, Xi'an 710119, China. [2]Institute of Biology and Medicine, College of Life and Health Sciences, Wuhan University of Science and Technology, Hubei 430081, P.R. China. [3]Wuhan No. 1 Hospital, Tongji Medical College, Huazhong University of Science and Technology, Wuhan 430022, Hubei, China. [4]Hematology-Oncology Division, Department of Medicine, BIDMC, Harvard Medical School, CLS-432, 330 Brookline Avenue, Boston, MA 02215, USA. [5]Li-Yang Wang and Ji Shi contributed equally to this work. ✉email: liangjiaqian4@qq.com; xinghualiao@wust.edu.cn; shaoyong_chen@hotmail.com

molecular mechanisms and actionable targets that could facilitate the development of alternative therapeutic strategies for CRPC. Recent years, RNA-editing offers a novel perspective with immense potentials to tackle various cancers[7–9], including PCa[10,11].

RNA-editing encompasses a range of post-transcriptional modifications that confers specific sequence alterations in RNA transcripts[12]. Two main RNA-editing types in mammals are based on adenosine (A) to inosine (I) (A-to-I) and cytosine (C) to uridine (U) (C-to-U) conversions[9], which are catalyzed by adenosine deaminases acting on RNA (ADAR) and apolipoprotein B mRNA-editing enzyme catalytic polypeptide (APOBEC) cytidine deaminases, respectively. In human cells, A-to-I RNA-editing[13] prevails in pre-mRNA splicing, translation and gene regulation, profoundly affecting RNA stability and biogenesis[9,12]. A-to-I editing has been extensively implicated in tumorigenesis, ADAR has consistently been identified as a promising therapeutic target in various cancers[14–16]. In comparison, C-to-U RNA-editing has been less extensively studied. The AID/APOBEC family enzymes mediate DNA editing by deaminating C-to-U in single-stranded DNA (ssDNA), leading to DNA damage such as base substitutions and strand breaks[17]. This mechanism is critical for immune defense against viral infections but also implicated in genomic instability and cancer-associated mutagenesis[18,19]. Notably, APOBEC3C and APOBEC3D have been shown to promote DNA replication stress resistance in pancreatic cancer cells by deaminating cytidines in the nuclear genome, thereby ensuring DNA replication fork restart and repair[20]. Moreover, APOBECs have been implicated in the regulation of mRNA stability and microRNA targeting[9]. Collectively, these suggested the involvement of APOBECs in cancer progression, potentially through the induction of mutations and genomic instability.

Accordingly, accumulating evidence have documented that RNA-editing plays a pivotal role in PCa development and progression[9–12]. Indeed, A-to-I editing of the AR has been reported to impair its interaction with androgenic or anti-androgenic ligands[10,12]. The prostate cancer biomarker gene *PCa antigen 3* (*PCA3*), a long non-coding RNA (lncRNA), was shown to regulate RNA-editing of the PCa suppressor PRUNE2 via ADARs and functions in PCa cell proliferation[11]. Additionally, the widespread alterations in RNA-editing patterns of human cancer have been annotated in The Cancer Genome Atlas (TCGA) database and 4 clinically relevant RNA-editing sites were detected in PCa[12].

The human genome encodes totally 19 genes that composes the adenosine and cytidine deaminase family[21]. The ADAR/ADAT genes are A-to-I editors that regulate RNA splicing and gene transcription; while the AID/APOBEC genes are C-to-U editors that engage with innate and adaptive immunity. The objectives of our current report are, for the first time, to comprehensively profile this gene family in typical PCa cell lines and clinical cohorts. We also aim to clarify whether AR mediates the transcription of this group of genes, including their responsiveness to AR agonists versus antagonists. These efforts would help to define the potential of targeting RNA editors in PCa intervention and expose novel diagnostic biomarker(s) and therapeutic target(s).

Results

The expression profile of RNA-editing related genes in prostate cancer

To systemically investigate the expression of RNA-editing family members in PCa, we profiled all 19 adenosine and cytidine deaminase genes with RNA-Seq datasets from the Cancer Dependency Map project (DepMap). This analysis was conducted across four typical prostate cell lines: Immortalized Prostate Epithelial Cells (PrEC-LH), Benign Prostatic Hyperplasia-1 cells (BPH-1), and two prostate adenocarcinoma cell lines (LNCaP and VCaP). The results revealed variations in transcript expression of the RNA-editing family genes across these cell lines (Fig. 1A). Among the ADAR family genes, ADAD1 and ADAD2 are extremely low in the above cell lines (Fig. 1A) and are also relatively low in clinical samples (Fig. 1B-C), in which ADAD2 has much less expression in primary PCa and metastatic CRPC than respective controls. In contrast, the ADARB2 transcript was higher in PCa cell lines than PrEC-LH and BPH-1 cells, and were similarly up-regulated in clinical PCa cohorts as compared to normal controls (Fig. 1B). For the cytidine deaminase family genes, AICDA, APOBEC1, APOBEC2, APOBEC3A, and APOBEC4 transcripts were extremely low across the above cell lines (Fig. 1A) and PCa clinical cohorts (Fig. 1B-C). Nevertheless, the APOBEC3A gene was expressed much higher in BPH-1 than LNCaP and VCaP cell lines (Fig. 1A).

To investigate potential synergistic relationships among RNA-editing enzyme genes, we analyzed the correlation in their expression patterns. Our results revealed that most RNA-editing enzymes genes did not exhibit significant correlations in their expression in both primary PCa and CRPC. In contrast, the APOBEC3 family genes, which are uniquely clustered within the same 22q13.1 chromosomal region (Table 1), showed a distinct and strong association in their expression patterns. These genes, known for their function in catalyzing C-to-U deamination on single-stranded DNA, exhibited positively correlated expression in both primary PCa and CRPC cohorts, with particularly strong correlations observed in CRPC (Fig. 2A-B). Furthermore, genetic analysis of the SU2C CRPC cohorts demonstrated that these APOBEC3 genes shared highly concordant chromosomal alterations, as exemplified in the pattern of gene amplification (Fig. 2C). This concordance is likely attributable to their physical linkage within the same chromosomal region, highlighting the coordinated nature of genomic alterations within the APOBEC3 cluster. These findings underscore the potential common regulatory mechanisms and potential common selection pressure among APOBEC3 family members. Among these APOBEC3 members, APOBEC3C emerged prominently as the most highly expressed cytidine deaminase gene in both primary PCa and CRPC (Fig. 1B-C). Of importance, APOBEC3C is less expressed in PCa cell lines (LNCaP and VCaP) than control lines (PrEC-LH and BPH-1) and in primary PCa than normal controls (Fig. 1A-B). The expression profiling of APOBEC3D and APOBEC3G mimicked that of APOBEC3C. Taken together, these findings delineated the expression of RNA-editing family genes in PCa typical cell lines and clinical samples.

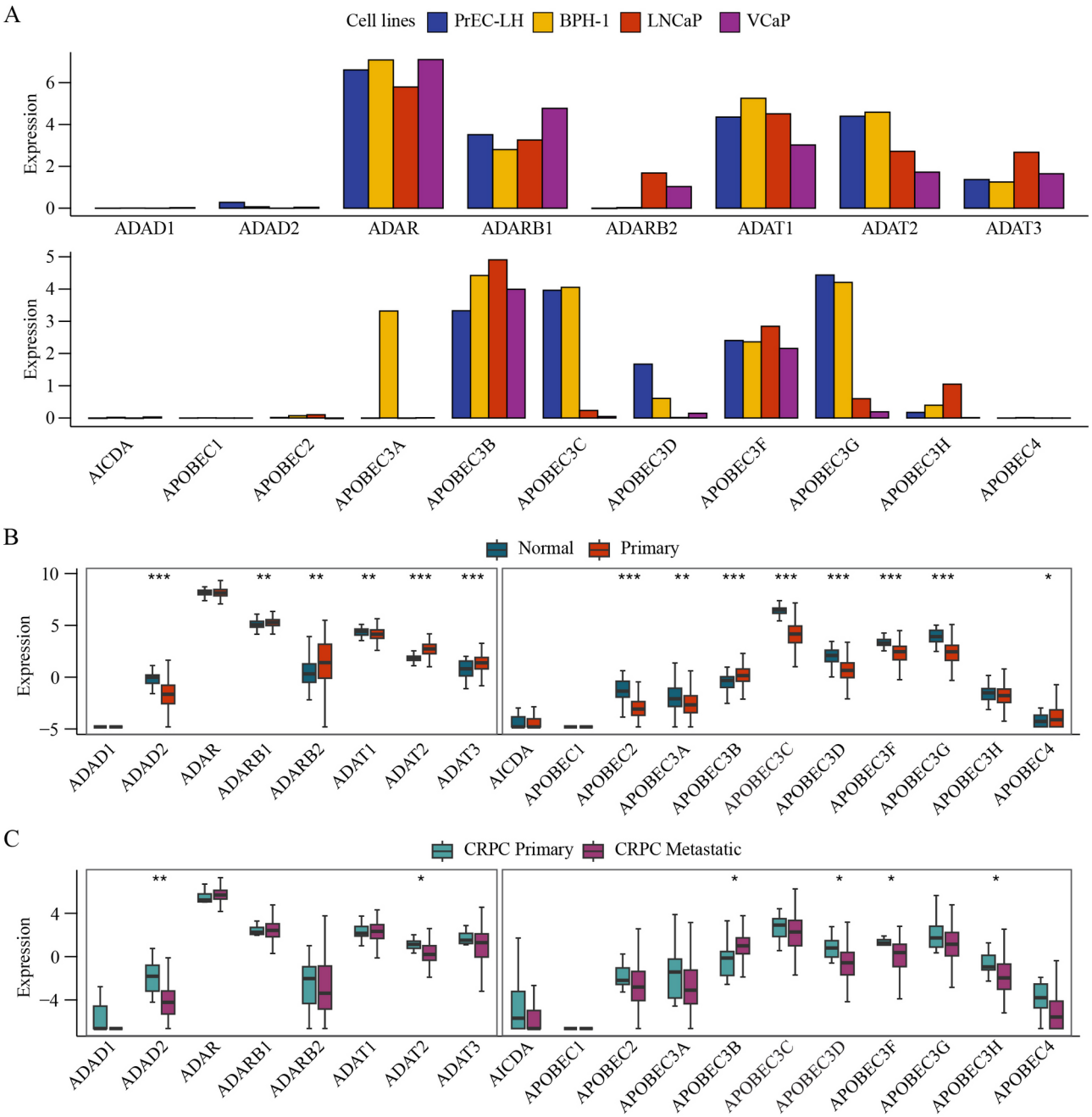

Fig. 1. Expression profiling of RNA-editing genes in typical prostate cell lines and clinical PCa cohorts. (**A**) The expression levels of 19 RNA editing genes across two type of benign prostate cells: immortalized prostate epithelial cells (PrEC-LH) and Benign Prostatic Hyperplasia-1 cells (BPH-1), as well as two prostate adenocarcinoma cell lines: LNCaP and VCaP. (**B**,**C**) Alignment of RNA-editing gene expression profiles in TCGA primary PCa cohorts versus normal samples (**B**), and in SU2C CRPC cohorts (primary CRPC versus metastatic CRPC) (**C**). Normal $n = 52$; primary PCa $n = 495$; primary CRPC $n = 7$; metastatic CRPC $n = 259$. * denotes $p < 0.05$, ** denotes $p < 0.01$, and *** denotes $p < 0.001$.

The down-regulation of APOBEC3C correlates with the progression of PCa

To further explore the clinical relevance of endogenous RNA-editing genes, we next assessed the expression profiles of 19 RNA-editing family members based on public PCa databases. Using TCGA prostate adenocarcinoma datasets, we applied the R package "limma" to examine expression of this gene sets (Fig. 3A). The computation process was based on filtering with an absolute log2 fold change (> 2) and a statistical significance (p-value of < 0.05). As shown, our analysis revealed that APOBEC3C, APOBEC3D, APOBEC3F, and APOBEC3G transcripts were significantly down-regulated in prostate adenocarcinoma tissues in comparison to normal prostate tissues, indicating potential tumor-suppressive functions.

Gene	Chromosome location	Enzymatic activity	Role in RNA editing
ADAR	1q21.3	Adenosine deaminase	Catalyzes the A-to-I RNA editing in dsRNA
ADARB1	21q22.3	Adenosine deaminase	Catalyzes the A-to-I RNA editing in dsRNA
ADARB2	10p15.3	Lacks editing activity	Prevents other ADAR enzymes to targets, and binds to both dsRNA and ssRNA
ADAT1	16q23.1	Adenosine-37 deaminase	Specifically deaminates A-37 to I in tRNA-Ala
ADAT2	6q24.2	Adenosine-34 deaminase	Probably deaminates A-34 to I in many tRNAs
ADAT3	19p13.3	Adenosine deaminase	Catalyzes the A-to-I RNA editing in tRNA
ADAD1	4q27	Adenosine deaminase	Catalyzes the A-to-I RNA editing in RNA, and bind exclusively to RNA, and is essential for male fertility and germ cell differentiation
ADAD2	16q24.1	Adenosine deaminase	
AICDA	12p13.31	Cytidine deaminase	Catalyzes the C-to-U conversion specifically during transcription of ssDNA
APOBEC1	12p13.31	Cytidine deaminase	Catalyzes the C-to-U post transcriptional editing of diverse mRNAs
APOBEC2	6p21.1	Low intrinsic cytidine deaminase activity	Probably deaminates C to U editing and involved in DNA demethylation
APOBEC3A	22q13.1	Cytidine deaminase	Deaminates both methyl-C and C to U, and selectively targets ssDNA
APOBEC3B			Deaminates C to U editing, selectively targets ssDNA and does not deaminate dsDNA, dsRNA or ssRNA
APOBEC3C			
APOBEC3D			
APOBEC3F			
APOBEC3G			
APOBEC3H			
APOBEC4	1q25.3	Cytidine deaminase	Putatively deaminates C to U editing

Table 1. The human adenosine and cytidine deaminase family members. *A* adenosine, *I* inosine, *C* cytidine; *U* uridine, *dsDNA/dsRNA* double-stranded DNA/RNA, *ssDNA/ssRNA* single-stranded DNA/RNA, *ADAR* adenosine deaminases acting on RNA.

Next, we assessed the prognostic potential of these 19 RNA-editing genes using univariate Cox regression analysis, by leveraging the clinical information in TCGA datasets. As shown, expressions of ADAT1, APOBEC2, APOBEC3B, APOBEC3C, and APOBEC3H had prognostic significance on PCa relapse (Fig. 3B), while APOBEC3C and ADAT2 obtained prognostic relevance on PCa overall survival (Fig. 3C). Notably, combined analyses exposed APOBEC3C as the sole RNA-editing gene that bore significance in both differential gene expression and PCa prognosis (Fig. 3D).

Collectively, by integrated analyses of multiple datasets that encompass both primary PCa and CRPC cohorts, we determined that APOBEC3C is markedly down-regulated in primary PCa (Figs. 1B and 3E-F); it is further down-regulated in more aggressive PCa specimens, compared to both normal and primary PCa tissues (Fig. 3G-H). These findings substantiated the reverse correlation of APOBEC3C with PCa oncogenesis and progression.

APOBEC3C is an AR transcriptionally repressed gene in PCa

PCa initiation and progression are tightly associated with the AR pathway, which drives a signature gene subset including KLK3 (prostate-specific antigen, PSA), a PCa diagnostic biomarker. AR-mediated cell-proliferative and oncogenic functions cover central metabolism programs and mTOR activation[1,22]. Next, we addressed AR-dependent regulation of these RNA-editing genes, with APOBEC3C as the concentration. We monitored the effects of AR agonists (dihydrotestosterone, DHT, and R1881) and antagonist (enzalutamide, ENZ) in public datasets and typical PCa cell lines. Specifically, in VCaP datasets GSE157107 and GSE135879, we observed that androgen activated canonical AR-signature genes (including KLK2, KLK3/PSA, etc.); while APOBEC3C expression was massively repressed (Fig. 4A-B). These findings were reproducible in the R1AD1 PCa cell lines (Fig. 4C-D). In comparison, APOBEC3C transcript was up-regulated by ENZ in R1AD1 cells, in opposite to the response of AR-signature genes (KLK2 and KLK3/PSA) (Fig. 4C-D).

The above observations in VCaP cells evidenced that APOBEC3C is an androgen-repressed gene. To further corroborate these findings, we examined public transcriptomes (GSE82223) of VCaP (Fig. 4E) and LNCaP (Fig. 4F) cells. In this dataset, both cell lines were subjected to DHT stimulation and AR knockdown with siAR. Indeed, in both cell lines DHT activated canonical AR-signatures but repressed APOBEC3C expression; in contrast, these androgen-mediated effects were effectively reversed by AR knockdown (Fig. 4E-F). For validation, we then performed RT-qPCR tests in VCaP cells that were subjected to DHT versus ENZ treatments (Fig. 4G). Indeed, APOBEC3C expression was repressed by DHT and enhanced by ENZ, with full-length AR (AR-FL, an AR-repressed gene[23] and KLK3/PSA (an AR-activated gene) as controls. Consistent with the findings in transcriptional regulation, Western blotting analysis further confirmed that APOBEC3C protein levels were down-regulated upon DHT treatment, in opposite to DHT-induced expression of KLK3/PSA proteins (Fig. 4H). Taken together, these findings validated AR-mediated repression of APOBEC3C gene in prostate cancer cells.

The above findings demonstrated androgen effects on APOBEC3C gene expression and next, we aim to clarify the direct engagement of AR in its transcriptional regulation. We first predicted putative AR-binding motifs across

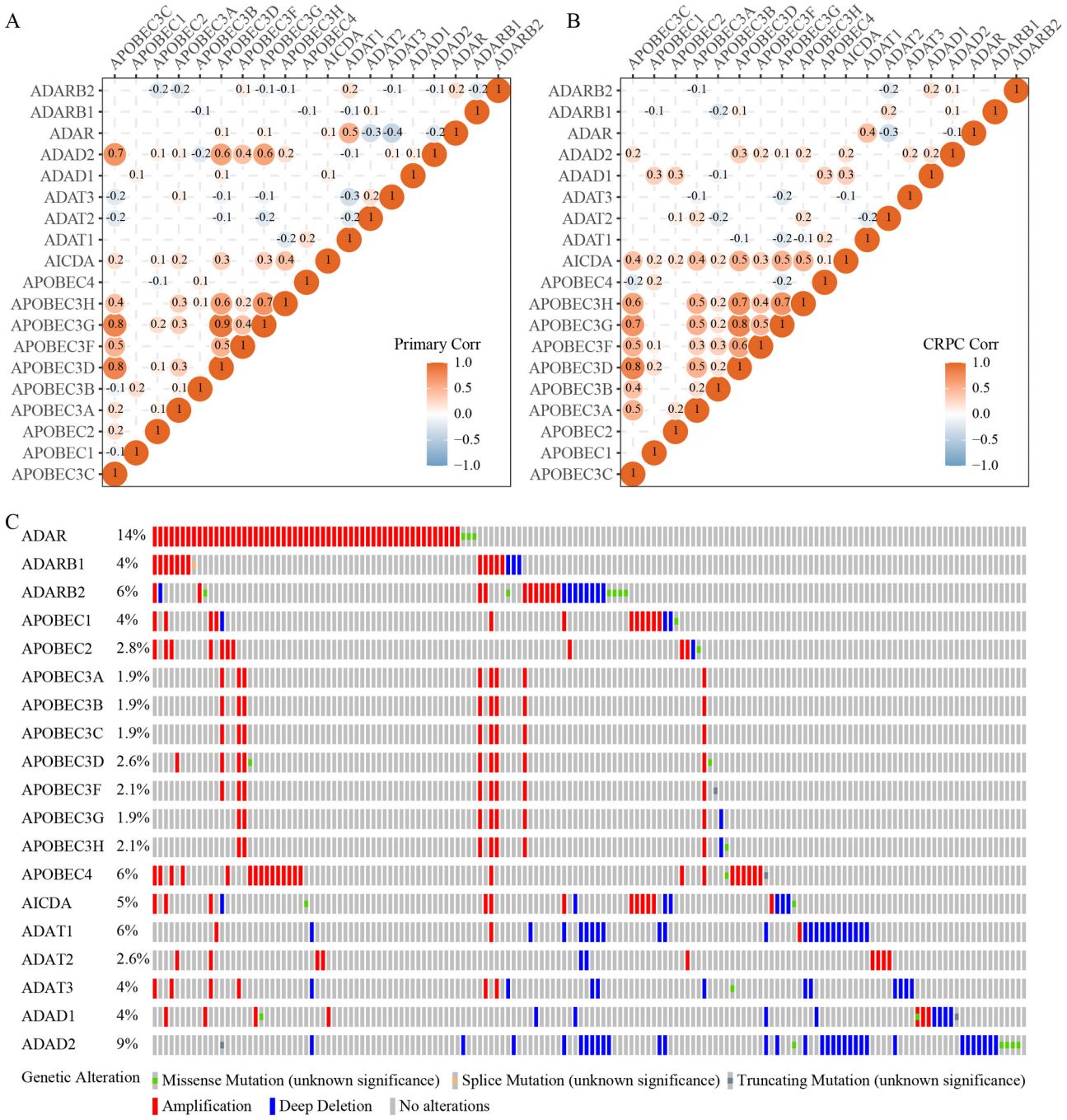

Fig. 2. Correlation of RNA editing genes in primary PCa and CRPC. (**A**,**B**) Pearson correlation coefficient matrix diagram of 19 RNA editing genes in TCGA primary PCa (**A**) and SU2C CRPC (**B**) cohorts. The values displayed represent precise significant correlations with p-values of 0.05 or less. The size and color intensity of circles are directly proportional to the respective Pearson coefficient, with red indicating a positive correlation and blue signifying a negative one. Additionally, insignificant results (p-values greater than 0.05) were omitted and represented by the absence of circles. primary PCa $n = 495$; metastatic CRPC $n = 259$. (**C**), Frequencies of chromosomal alteration for the RNA-editing genes based on analysis of the SU2C CRPC cohorts in the cBioPortal database ($n = 429$).

the APOBEC3C locus using JASPAR database (Matrix ID: MA0007.2; AR motif score > 85); through integrative analysis of AR and H3K27ac (marking epigenetically active chromatin) ChIP-Seq datasets, we localized three candidate AR binding sites: site 1 and site 3 in the 5' region, and site 2 in the 3' region of APOBEC3C gene locus (Fig. 5A-B). To validate these predictions, we performed chromatin immunoprecipitation (ChIP) followed by quantitative PCR (qPCR) in LNCaP and VCaP cells cultured in androgen-containing medium. In accordance with AR ChIP-Seq profiling, ChIP-qPCR in LNCaP and VCaP cells grown in androgen-containing medium

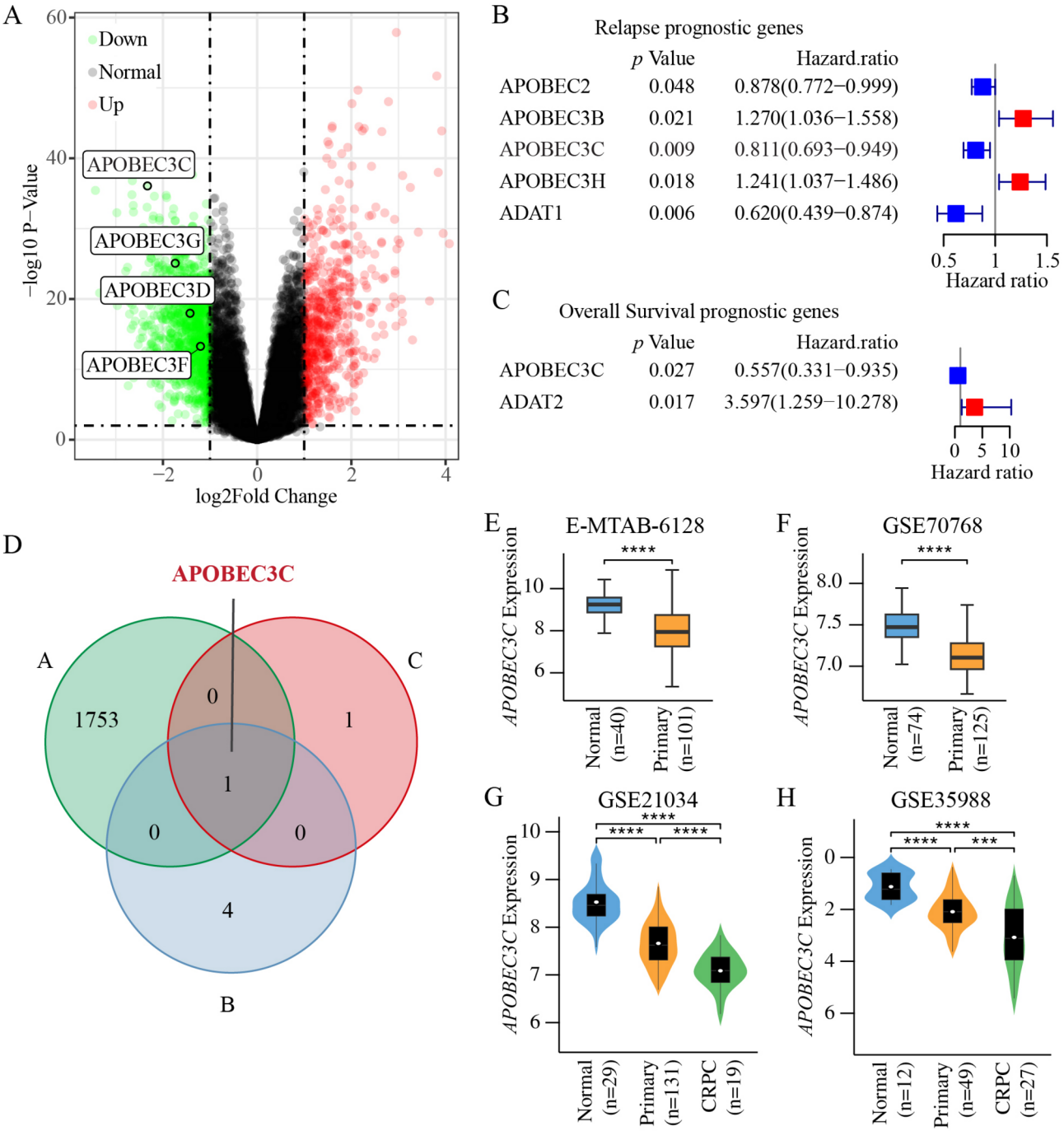

Fig. 3. Assessment of differenced expressed RNA editing genes and their prognostic significance in PCa. (**A**) Volcano plot of differently expressed genes (DEGs) between normal and prostate adenocarcinoma samples based on TCGA datasets, in which the RNA editing DEGs were highlighted. (**B**,**C**) Forest plot of hazard ratio for relapse (**B**) and overall survival (OS, (**C**)) associated prognostic RNA editing genes in PCa. (**D**) Venn diagram on the overlap between DEGs (**A**) and prognostic genes on PCa relapse (**B**) and OS (**C**). APOBEC3C stood out as the only RNA-editing DEG having prognostic significance. (**E**,**F**), Box plots of APOBEC3C expression in primary PCa versus normal controls (based on E-MTAB-6128 and GSE70768). (**G**,**H**) Violin plots of APOBEC3C expression in primary PCa and CRPC versus normal controls (based on datasets GSE21034 and GSE35988, respectively). *** denotes $p < 0.001$, and **** denotes $p < 0.0001$.

confirmed significant AR enrichment at sites 1 and 2 as compared to site 3, with the site 2 having the strongest AR occupancy. In comparison, the PSA-enh has enriched AR occupancy while the non-specific site (NS) does not (Fig. 5C-D).

In VCaP cells, DHT increased AR binding at the APOBEC3C gene 3' enhancer site (as marked by the peak of H3K27ac) and significantly, H3K27ac occupancy was massively reduced by androgen, consistent with AR-mediated transcriptional repression activity (Fig. 5A, Fig. S1A). In LN95 PCa cells, AR activities were attenuated by ARCC-32, a competitive AR degrader (ARD)[2]. As shown, in LN95 cells AR chromatin binding at the APOBEC3C gene 3' sites were effectively abrogated by siAR treatment, as compared to the siGFP control (Fig. S1B). Of importance, we verified that ARD depleted AR proteins but enhanced APOBEC3C expression (Fig. S1C-D). Additionally, we analyzed the expression profiles of APOBEC3C in PCa cell lines encompassing distinct AR signaling contexts (PC3: AR-null, DU145: AR-null, LNCaP: AR-sensitive, and VCaP: CRPC-derived AR-active), based on DepMap portal (Fig. S1E) and RT-PCR verification (Fig. S1F). Our results demonstrated that AR-negative PC3/DU145 cells exhibited higher baseline levels of APOBEC3C compared to AR-positive LNCaP/VCaP cell lines. These findings provide further insight into the regulation of APOBEC3C across different PCa models. Collectively, our findings established AR-mediated APOBEC3C-repression mechanism: Upon androgen stimulation, AR-FL directly binds to APOBEC3C gene locus (particularly the 3' enhancer site) and represses its transcription via epigenetic chromatin inactivation (as marked by decrease in H3K27ac).

The expression of APOBEC3C and AR-signature genes is in reverse correlation in PCa clinical cohorts

To define APOBEC3C in AR-mediated transcriptional network, we next focused on multiple datasets derived from PCa clinical cohorts. As expected, an analysis of the GSE48403 datasets verified that androgen deprivation therapy (ADT) resulted in the down-regulation of AR-activated gene sets, including KLK2, KLK3/PSA, NKX3-1, TMPRSS2, FKBP5, ZBTB16 and SORD (Fig. 6A-B and S2A-E). In contrast, ADT led to pronounced up-regulation of APOBEC3C expression in clinical samples (Fig. 6C). Notably, assessment of APOBEC3C protein expression in PCa pathological specimens revealed its reverse correlation with KLK3/PSA protein levels. Specifically, in comparison to the benign controls, PCa tumor samples exhibited gain in KLK3/PSA protein expression (marking the activation of AR-dependent transcriptional pathway) but attenuation in proteins of APOBEC3C (Fig. 6F), upholding its negative regulation by AR. Intriguingly, while up-regulation by ADT occurred on a majority of APOBEC family members (APOBEC3C, APOBEC3F, and APOBEC2, which catalyze C-to-U editing), an opposite trend was noted on a panel of ADAR family members (ADARB1, ADARB2, and ADAT1, which catalyze A-to-I editing) (Fig. 6C and S2F-J).

We took further efforts to profile APOBEC3C expression upon clinical administration of AR antagonists. By referencing the CTRP and CellMiner datasets, we performed a predictive analysis on drug sensitivity in TCGA PCa cases with Abiraterone (Abr) and Enzalutamide (ENZ) treatments. Indeed, PCa patients with low APOBEC3C expression levels were more resistant to Abr and ENZ (Fig. 6D-E). Furthermore, calculation of TCGA primary PCa and SU2C CRPC datasets demonstrated that APOBEC3C expression was reversely correlated with AR-signature gene programs in primary PCa and obviously, this reverse correlation became even stronger in CRPC (Fig. 6G-H). Furthermore, by integrating datasets from primary and advanced PCa cases, we observed that the APOBEC3C gene locus exhibited decreased binding of AR and H3K27Ac at the 5' site and increased binding at the 3' site (Fig. 6I). It is conceivable that this mechanistic transition may contribute to APOBEC3C down-regulation during PCa development and progression. Notably, these findings were consistent with our observations in the VCaP cells (derived from a metastatic lesion of a CRPC patient[24], which exhibited prominent AR and K3K27Ac binding at the 3' site of APOBEC3C gene (Fig. 5A), in alignment with the profiles in the clinical metastasis (M) specimens (Fig. 6I). Additionally, an alignment of ATAC-seq (marking chromatin openness) further revealed massive reduction in the overall chromatin accessibility. In fact, the decline in chromatin openness occurred across the entire loci hosting the APOBEC3 family genes (Fig. S2K). Collectively, these findings highlighted the potential of APOBEC3C as an AR-repressed PCa candidate tumor suppressor and a biomarker for predicting Abr and ENZ responsiveness.

The clinicopathological profiles and prognostic significance of APOBEC3C in PCa

To further define the prognostic values of APOBEC3C along PCa progression, we then evaluated the correlation between APOBEC3C transcript and clinicopathological characteristics in TCGA datasets. Accordingly, the PCa patient cohorts were classified into five categories in accordance with the 2019 International Society of Urological Pathology (ISUP) Consensus Conference on Grading of Prostatic Carcinoma[25]. The disease stage of each case was assigned based on the guidance in the Eighth Edition of the AJCC Cancer Staging Manual[26]. As shown, we observed insignificant difference in APOBEC3C expression between Grade-I ($n=45$), Grade-II ($n=145$) and Grade-III ($n=101$) cohorts; however, the Grade-IV ($n=63$) and Grade-V ($n=141$) cases displayed substantially lower APOBEC3C expression (Fig. 7A). This pattern was consistently observed across PCa stages, as patients with more advanced stages (III-IV, $n=313$) had much less APOBEC3C transcript in comparison to those in earlier stages (I-II, $n=132$) (Fig. 7B).

Upon accessing the pathological stages, we next uncovered that the manifestation of lymph node metastasis (classified by N stages) did not exhibit a statistically meaningful association with APOBEC3C expression (Fig. S3A). In contrast, PCa distant metastasis (categorized by M stages) obtained lower APOBEC3C expression in the M1 stage cohorts ($n=3$) than that in the M0 stage cases ($n=453$) (Fig. S3B). However, the statistical significance of this finding was limited by the small sample size of the M1 group. The data from GSE41408 further demonstrate that metastatic PCa patients ($n=9$) exhibit significantly lower APOBEC3C expression compared to non-metastatic cases ($n=39$) (Fig. S3C). Nevertheless, PCa cohorts of the advanced T3-4 stages ($n=301$) indeed displayed markedly less APOBEC3C expression than those in the T1-2 stages ($n=187$) (Fig. 7C). Notably,

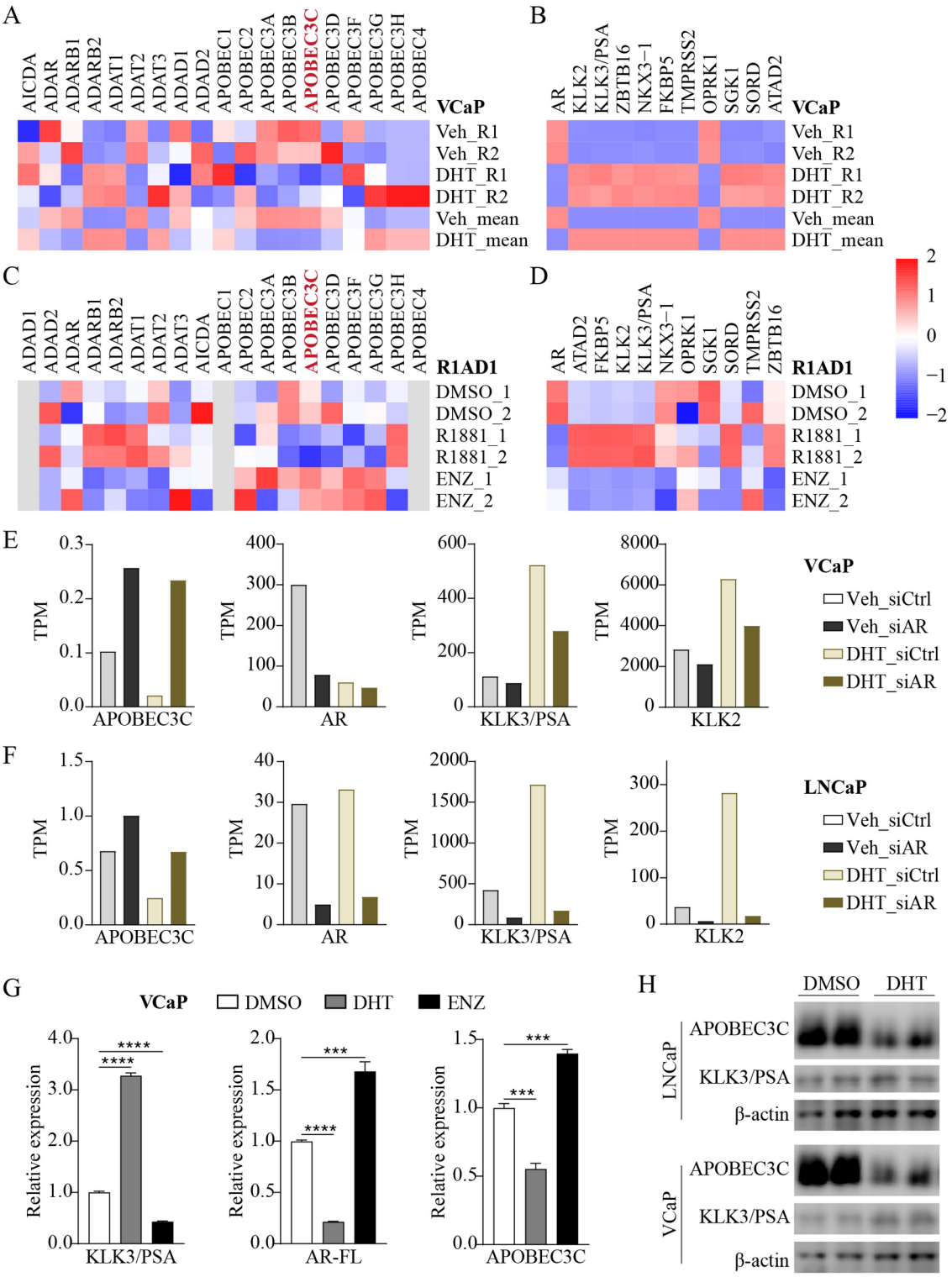

APOBEC3C transcripts were also reversely linked with the PSA gene expression; as shown, APOBEC3C mRNA was substantially lower in patients with PSA expression exceeding 20 ng/ml ($n = 54$) and between 10 and 20 ng/ml ($n = 97$), in comparison to those with PSA levels below 10 ng/ml ($n = 324$) (Fig. 7D). Collectively, these results uphold the AR-mediated APOBEC3C repression mechanism, its potential tumor suppressor status during PCa progression, and its biomarker potentials on disease malignancy.

To solidify the prognostic significance of the APOBEC3C gene, we next stratified TCGA PCa cohorts based on APOBEC3C expression levels, in annotation with patient survival status and relapse outcome. As shown, a strong reverse correlation was noted between APOBEC3C expression and PCa relapse and mortality incidences (Fig. 7E). These findings were further ratified by Kaplan-Meier analysis, in which patients were segregated into APOBEC3C high versus low expression cohorts. As shown, the APOBEC3C-low group obtained significantly unfavorable relapse-free survival probabilities (Fig. 7F). Additionally, these reverse correlations were validated

◀**Fig. 4**. Characterization of APOBEC3C as an AR-repressed gene in PCa. (**A**,**B**) Heatmap of mRNA expression profiles of the RNA-editing genes (**A**) and AR-signature genes (**B**) in VCaP cells, upon treatment with androgen (DHT) versus vehicle control (Veh). The analyses were based on datasets GSE157107. (**C**,**D**) Heatmap visualization of RNA-editing enzyme gene expression (**C**) and AR pathway signature gene expression (**D**) in R1AD1 cells under three treatment conditions: vehicle control (Veh), synthetic androgen R1881 stimulation, and enzalutamide (ENZ) suppression. Data derived from reanalysis of the GSE135879 dataset. (**E**,**F**) The expression of APOBEC3C, AR, and KLK3/PSA transcripts in VCaP (**E**) and LNCaP (**F**) cells, without or with AR knockdown (siAR versus siCtrl) and androgen (DHT versus vehicle). The analyses were based on datasets GSE82223. (**G**) RT-qPCR assay of APOBEC3C, AR-FL and KLK3/PSA (as normalized to actin) in VCaP cells that were exposed to DHT, ENZ, or vehicle control. (**H**) Protein expression levels of APOBEC3C and KLK3/PSA in LNCaP and VCaP PCa cell lines with DHT stimulation. *** denotes $p < 0.001$, and **** denotes $p < 0.0001$.

by external PCa datasets as well (Fig. S3D-K). However, overall survival (OS) analysis showed less compelling differences between the APOBEC3C high versus low groups, likely owing to the limited number of cases in our study (Fig. 7G). This constraint may obscure more definitive associations between APOBEC3C expression with OS and survival probabilities (Fig. 7E and G). Nevertheless, to quantitatively evaluate APOBEC3C on PCa diagnosis, we then conducted the ROC curve analysis that provided unequivocal evidence that APOBEC3C had the best diagnostic performance among 19 RNA-editing genes (Fig. 7H).

Discussion

Our comprehensive analysis of the 19 RNA-editing family genes revealed distinct expression patterns across PCa cell lines and clinical samples, highlighting their diverse and potentially critical roles in prostate tumorigenesis. Among these genes, APOBEC3C emerges as the most highly expressed cytidine deaminase gene in both primary PCa and CRPC. Remarkably, APOBEC3C distinguished itself as the only RNA-editing gene that gained significant relevance in both differential gene expression and PCa prognosis. Interestingly, while APOBEC3C exhibits genomic amplification in few CRPC cases (1.9%), its overall transcriptional level is decreased. This may be explained by persistent AR signaling in CRPC and additional regulatory mechanisms, including genomic, epigenetic, and post-transcriptional alterations. These factors likely account for why APOBEC3C expression remains down-regulated in CRPC patients despite ADT, indicating a complex regulatory mechanism that deserves further exploration. Notably, our results highlight APOBEC3C as an RNA-editing gene with the best diagnostic performance and a crucial candidate tumor suppressor in PCa.

Mechanistically, AR binds to the APOBEC3C gene locus and represses its transcription by inducing chromatin remodeling, as evidenced by reduced H3K27ac signals. Our finding revealed that APOBEC3C, which is not a known transcription factor, is significantly down-regulated in both primary PCa and CRPC, and its expression negatively correlates with AR signature gene sets. Clinically, reduced APOBEC3C expression correlates with advanced PCa stages, higher PSA levels, and worse relapse-free survival rates, underscoring its potential as both a prognostic biomarker and a predictor of therapeutic response. Notably, patients with low APOBEC3C levels showed resistance to AR antagonists, as exemplified by Abiraterone and Enzalutamide, indicating its potential utility in patient stratification for targeted therapy.

With the functional significance of AR splicing variants (in particularly ARv7) in sight, our findings showed APOBEC3C gene is repressed by the AR-FL, as evidenced by its up-regulation by AR knock-down, DHT-mediated repression in LNCaP (no detectable ARv7) and VCaP (low ARv7 that becomes even lower under androgen)[27], and up-regulation by AR degrader that specifically targets AR-FL. Nevertheless, the functions of AR variants in APOBEC3C gene regulation should be systemically assessed in future work, particularly in the settings of CRPC cells that highly express endogenous variants.

Previous studies have suggested roles for RNA-editing enzymes in various cancers, including PCa. However, this study is the first to comprehensively profile the entire RNA-editing gene family in PCa and specifically identify APOBEC3C as a candidate tumor suppressor. Unlike prior research that primarily focused on ADAR enzymes, our work highlights the understudied APOBEC family, particularly APOBEC3C. Our findings of AR-mediated transcriptional repression of APOBEC3C and its association with PCa progression and treatment response offer new insights into PCa oncogenesis and progression.

DNA editing has already revolutionized the biopharmaceutical sector, but RNA editing could prove to be equally powerful, granting new routes towards safer and redosable therapeutics[28,29]. RNA-editing drugs, specifically ADAR-based editors, have been advancing into clinical trials. Indeed, they offer new treatment options for rare genetic and complex diseases[30]. Research is also exploring broader RNA-editing pipelines beyond A-to-I editing, potentially incorporating other cellular editing systems. Nevertheless, targeting RNA-editors would offer advantages like redosability and different dosing schedules to PCa therapy. Given the profound diagnostic potential of APOBEC3C, we would suggest further exploring therapeutic strategies in the context of its transcriptional repression by AR and identify modalities that enhance its enzymatic activity.

Conclusions

In conclusion, our study offers a comprehensive characterization of RNA-editing genes in PCa and establishes APOBEC3C as a pivotal candidate tumor suppressor. The progressive down-regulation of APOBEC3C in PCa, driven by AR-mediated repression, highlights its central role in prostate tumor biology.

Our findings carry significant implications for PCa diagnostics and therapeutics, suggesting that APOBEC3C could be utilized as a robust biomarker for disease prognosis, therapeutic resistance, and potential patient

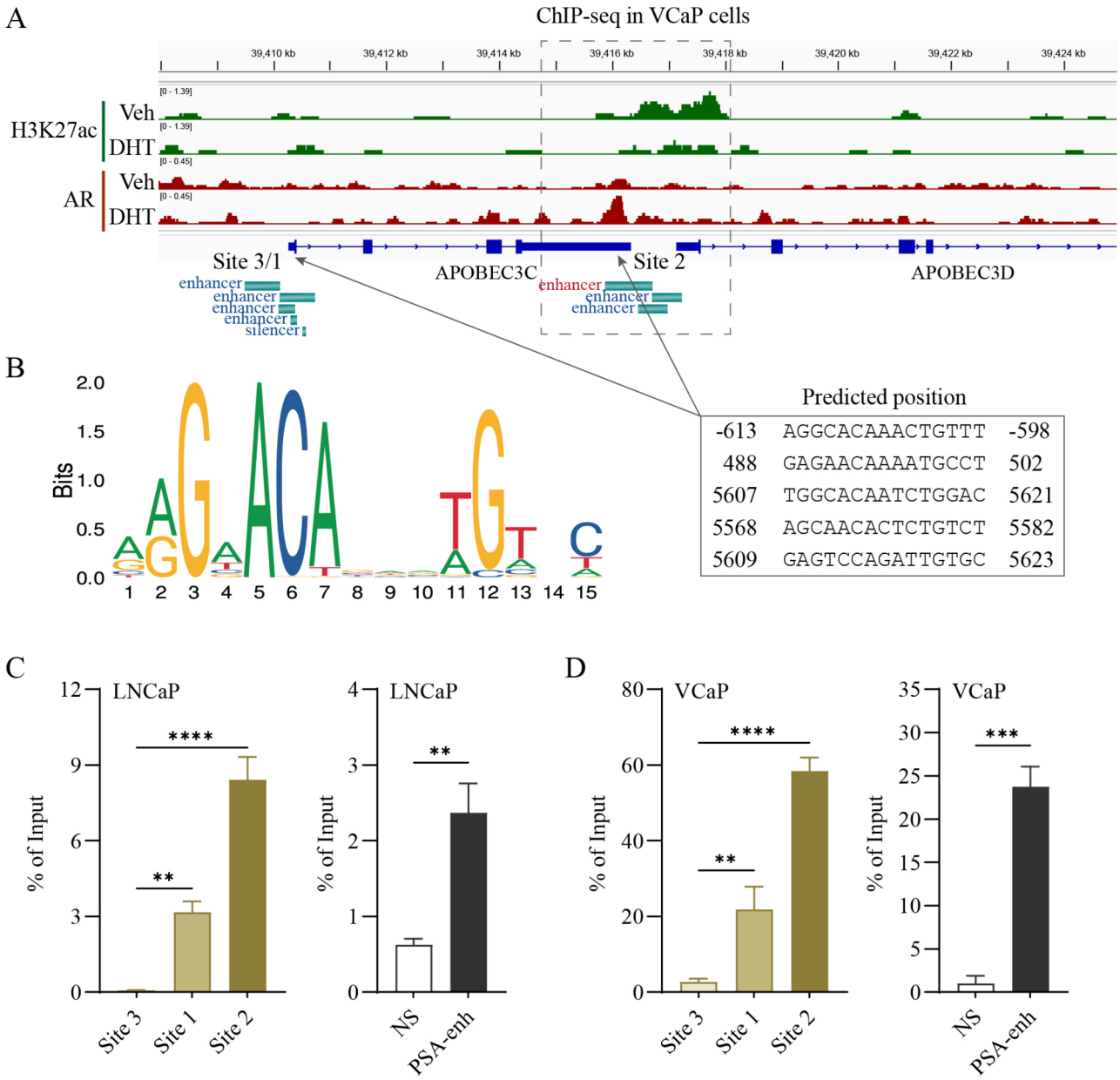

Fig. 5. Prediction and verification of AR binding sites in APOBEC3C. (**A**) Track visualization of H3K27ac and AR ChIP-seq peaks in the APOBEC3C gene locus (VCaP cells, DHT versus vehicle). (**B**), JASPAR prediction of AR binding motifs (Matrix ID: MA0007.2) within AR ChIP-seq peaks of the APOBEC3C locus. Left: AR consensus sequence; right: predicted binding positions. (**C**,**D**) ChIP-qPCR validation of AR occupancy at candidate sites (sites 1–3) in LNCaP and VCaP cells that were culture in androgen-containing medium (10% FBS). Controls: KLK3/PSA-enhancer (PSA-enh, ARE3) (positive control); NS (non-specific site, negative control). ** denotes $p < 0.01$, *** denotes $p < 0.001$, and **** denotes $p < 0.0001$.

stratification. Further investigations are needed to elucidate the mechanistic pathways regulated by APOBEC3C and to design therapeutic approaches aimed at restoring its tumor-suppressive activity in PCa.

Methods

Cell culture and reagents

PC3, DU145 and VCaP cells were grown in DMEM medium (Gibco, Cat. 12100046) supplemented with 10% fetal bovine serum (FBS, Gibco, Cat. A5670701) and 1% penicillin/streptomycin (P/S, HyClone, Cat. SV30010). LNCaP95 (LN95) cells were maintained in phenol-red-free RPMI1640 medium (HyClone, Cat. 118035-030) with 5% charcoal/dextran stripped FBS (CDS, HyClone, Cat. SH30068.03) and 1% P/S. All cells were incubated at 37℃ in a humidified incubator with 5% CO_2. For compound treatment, VCaP cells were exposed to androgen (dihydrotestosterone, DHT, 10 nM, Selleck, Cat. S4757) versus Enzalutamide (ENZ, 10 μm, Selleck, Cat. S1250)

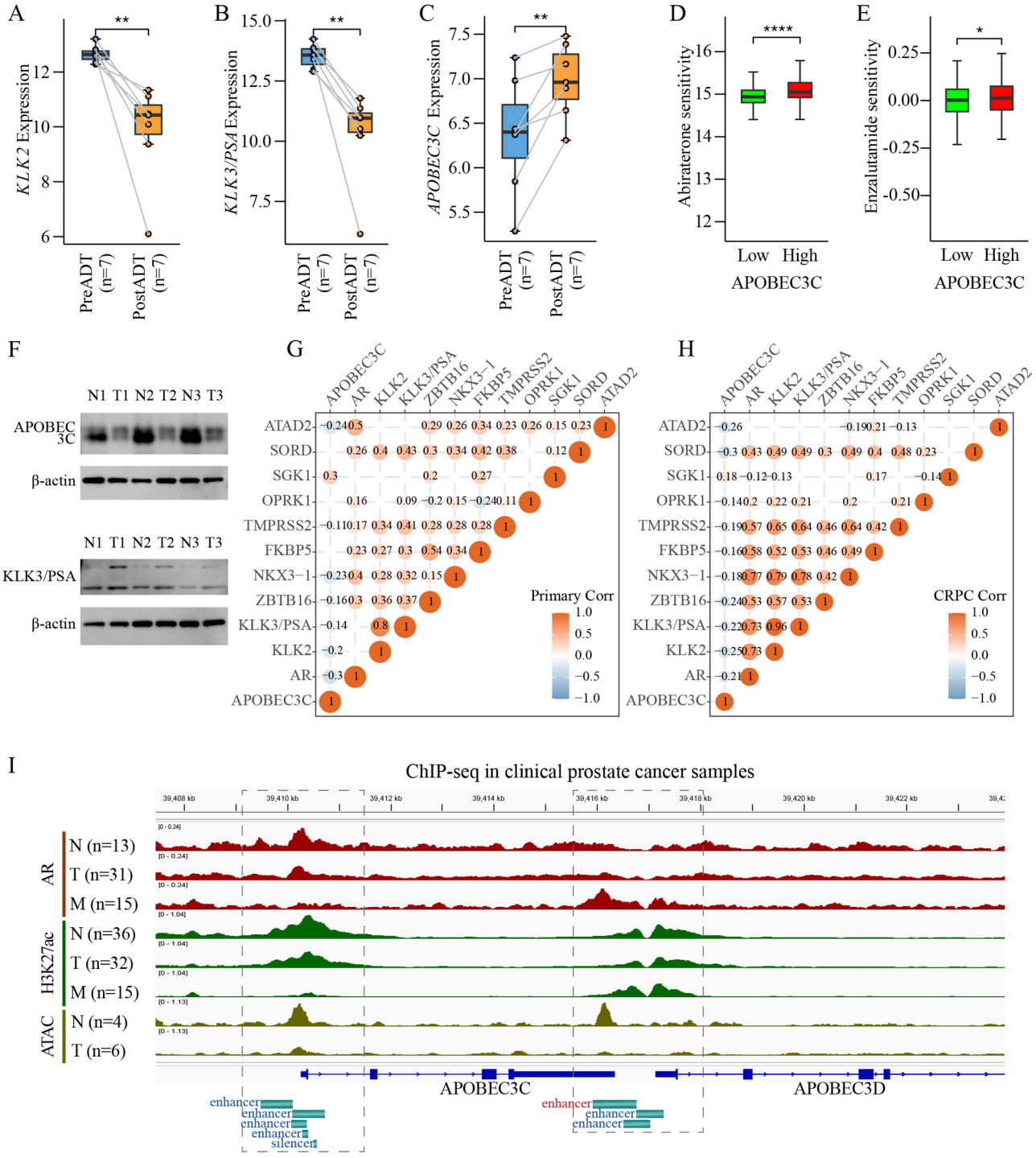

Fig. 6. Characterization of APOBEC3C as an AR-repressed gene in clinical PCa cohorts. (**A**-**C**) The expression profiles of KLK2, KLK3/PSA and APOBEC3C in clinical PCa samples. This comparison was based on paired samples from each individual patient (before and after the androgen deprivation therapy (ADT)). The analyses were based on the datasets GSE48403. (**D**-**E**) An alignment between APOBEC3C expression levels and the sensitivity to abiraterone (Abr, (**D**)) and enzalutamide (ENZ, (**E**)) in PCa patients, based on TCGA, CTRP2 and CellMiner datasets. (**F**) Protein expression levels of APOBEC3C and KLK3/PSA in PCa pathological specimens (T1, T2 and T3) and benign controls (N1, N2 and N3). (**G**,**H**), Pearson correlation coefficient matrix diagram between APOBEC3C and AR-signature genes in TCGA primary PCa (G) and SU2C CRPC (**H**) cohorts, respectively. (**I**) Track visualization of AR and H3K27ac ChIP-Seq and ATAC-seq peaks in the APOBEC3C gene locus in clinical PCa samples, which were categorized into three groups: normal (N), primary PCa (T) and metastatic CRPC (M). The analyses were based clinical PCa datasets GSE130408 and GSE70079, the bigWig files of all cases within each group were normalized, merged and then averaged. * denotes $p < 0.05$, ** denotes $p < 0.01$, and **** denotes $p < 0.0001$.

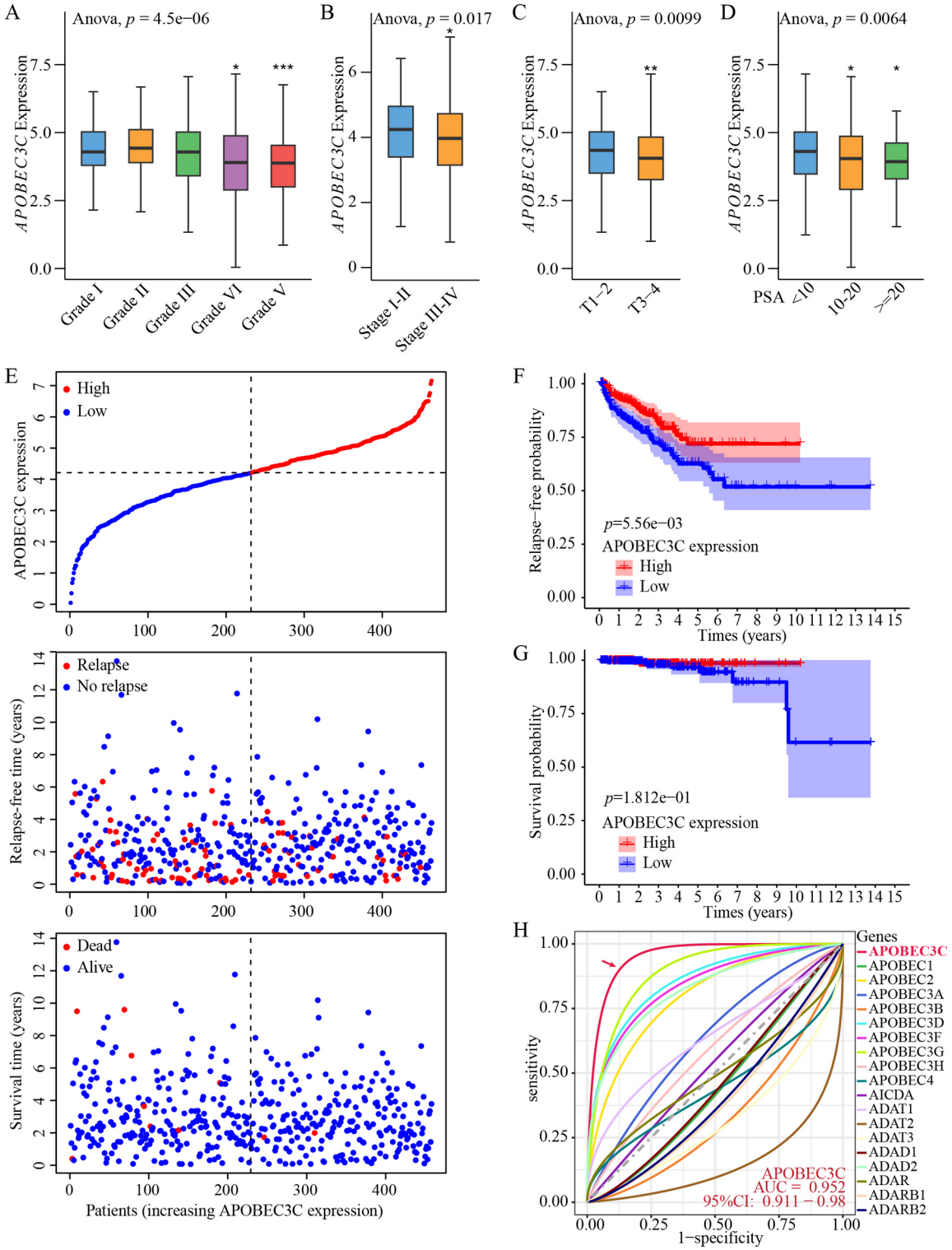

Fig. 7. The clinicopathological profile and prognostic significance of APOBEC3C in PCa clinical cohorts. (**A**-**D**) The profile of APOBEC3C expression in TCGA primary PCa cohorts, classified by tumor grade (**A**), stage (**B**), pathological T stage (**C**), and PSA level (**D**). (**E**) Relapse and survival distributions of PCa patients stratified along APOBEC3C transcript levels. (**F**,**G**) Kaplan-Meier curves of relapse-free survival (RFS, **F**) and overall survival (OS, **G**) analyses in TCGA primary PCa cohorts, with patients stratified into APOBEC3C high ($n = 232$) versus low ($n = 232$) expression groups. (**H**) Graph of receiver operating characteristic (ROC) curves that represents the predictive accuracy of RNA-editing gene expression on PCa prognosis. * denotes $p < 0.05$, ** denotes $p < 0.01$, and *** denotes $p < 0.001$.

for 24 h. LN95 cells were treated with AR degrader ARCC-32 (100 nM, Arvinas Operations) for 12 h for further analysis. Vehicle (DMSO) was used as the control. All cell lines have been tested for mycoplasma contamination before conducting the experiments.

Quantitative real-time PCR (RT-qPCR) assay

Total RNA was extracted with the TRIzol reagent (Invitrogen, Cat. 15596018), in accordance with the manufacturer's instruction. Subsequently, 1 μg of total RNA was reverse transcribed into complementary DNA (cDNA) using the PrimeScript™ RT Master Mix kit (Takara, Cat. RR036A), following the manufacturer's protocol. PCR amplification was performed using TB Green Premix Ex Taq II kit (Tli RNaseH Plus, Takara, Cat. RR820A) along with specific primers. The primer sequences (5' to 3') were listed as below: Actin - forward: GCT ATCCAGGCTGTGCTATC, reverse: TGTCACGCACGATTTCC; AR-FL - forward: ACATCAAGGAACTCGA TCGTATCATTGC, reverse: TTGGGCACTTGCACAGAGAT; KLK3/PSA - forward: TCTGCGGCGGTGTTC TG, reverse: GCCGACCCAGCAAGATCA; APOBEC3C - forward: CTTGGTTCTGCGACGACATAC, reverse: TCCTGGTAACATGGATACTGGAA. The RT-qPCR reaction was conducted on a CFX96 Real-Time System (Bio-Rad). It starts an initial denaturation step at 95 °C for 3 min, followed by 40 cycles of amplification (95 °C for 30 s plus 60 °C for 30 s). Relative gene expression was calculated based on $2^{-\Delta\Delta CT}$, with the housekeeping gene actin as internal control for normalization.

Chromatin immunoprecipitation (ChIP) assay

Chromatin immunoprecipitation was performed using the ChIP Assay Kit (Beyotime Biotechnology, Cat. P2078). Cells were cross-linked with 1% methanol for 10 min at 37 °C, followed by quenching with glycine (10X solution) for 5 min. After PBS washes, cells were lysed in SDS Lysis Buffer on ice for 10 min. Chromatin fragmentation was achieved by sonication using a Bioruptor® system (10 s ON/10 sec OFF, 25 W power, 15 cycles at 4 °C). Fragmented DNA (200 μL) was size-verified by agarose gel electrophoresis after phenol-chloroform extraction. The remaining chromatin was diluted in ChIP Dilution Buffer, pre-cleared with Protein A/G Agarose for 30 min on ice, and incubated overnight at 4 °C with AR antibodies (1:100, Proteintech, Cat. 66747-1-PBS). Immune complexes were captured using Protein A/G Agarose for 1 h on ice, washed sequentially with Low Salt Immune Complex Wash Buffer, High Salt Immune Complex Wash Buffer, and TE Buffer, then eluted with Elution Buffer. Crosslinks were reversed by incubating with NaCl at 65 °C for 4 h. Purified DNA was analyzed by qPCR using primers specific to a non-specific control site (NS: forward 5′-CAGAGGGCTTCTGGTGC-3′, reverse 5′-TTGACAATGTCTTGCCTTGG-3′), KLK3/PSA-enhancer (ARE3) (PSA-enh: forward 5′-GCCTG GATCTGAGAGAGATATCATC-3′, reverse 5′-ACACCTTTTTTTTTCTGGATTGTTG-3′), and APOBEC3C regions (site1: forward 5′-GGAGGGGCCATGATTCACAA-3′, reverse 5′-CGTGCAGAGGTACCTGATCT-3′; site2: forward 5′-GTGTTGCTCCTCTTGTCCA-3′, reverse 5′-GCAGAAGAATCGCTTAAACTCG-3′; site3: forward 5′-AGTTTGTGCCTTCAGTCTC-3′, reverse 5′-ATCCCCTCTTCCAACCTC-3′).

Quantitative analysis was performed using the formula:

$$\text{Percentage of Input} = 5\% \times 2^{\left({}^{\text{CT}}{}_{\text{Input}} - {}^{\text{CT}}{}_{\text{ChIP}}\right)}$$

where CT_{Input} and CT_{IP} represent the threshold cycle values of the input DNA and immunoprecipitated DNA, respectively. This calculation accounts for the 20-fold dilution factor of input DNA (5% = 1/20). PCR conditions included an initial denaturation at 95 °C for 3 min, followed by 40 cycles of 95 °C for 30 s and 60 °C for 30 s on a CFX96 Real-Time System.

Western blotting (WB) assay

Cells lysis was performed using the RIPA buffer (150mM NaCl, 10mM Tris-HCl (pH 7.2), 0.5% SDS, 1% NP-40, 0.5% deoxycholate) with fresh Halt Protease Inhibitor Cocktail (Thermo Fisher, Cat. 78438). Total proteins were normalized and resolved with 4–12% Criterion™ XT Bis-Tris Protein Gel (Bio-Rad, Cat.3450123). Upon transfer onto 0.2 μm Nitrocellulose Membrane (Bio-Rad, Cat. 1704271), the blots were blocked with 5% nonfat dry milk in Tris-buffered saline containing 0.05% Tween-20 (TBST) for 1 h at room temperature, and then incubated for overnight at 4℃ with primary antibodies on an orbital shaker. After washing with TBST, the membranes were next blotted with secondary antibody conjugated with horseradish peroxidase for 1 h at room temperature. Finally, the blots were developed with ECL luminescence reagent (Bio-Rad, Cat. 1705061) on an automated chemiluminescence image analysis system. The primary antibodies used in this study were for APOBEC3C (1:1000, Proteintech, Cat. 10591-1-AP), KLK3/PSA (1:1000, Proteintech, Cat. 10679-1-AP), AR (1:1000, Abcam, Cat. ab74272) and beta-actin (1:1000, β-actin, Santa Cruz, Cat. sc-69878).

Tissue lysis

Freshly dissected tissue samples were cut into pieces and homogenized in ice-cold RIPA lysis buffer (supplemented with protease inhibitor cocktail and PMSF) using a pre-chilled mortar and pestle. The homogenate was subjected to pulsed ultrasonication on ice three times, followed by centrifugation at 12,000 × g for 15 min at 4 °C to collect the supernatant. Protein concentration was determined using the BCA assay, and lysates were normalized to 3 μg/μL with RIPA buffer before adding 5× Laemmli loading buffer. Samples were denatured at 95 °C for 10 min in a thermal block and stored at -20 °C for short-term use or -80 °C for long-term preservation.

Data collection

The gene expression and clinical information of primary PCa and CRPC patients were retrieved from The Cancer Genome Atlas (TCGA) database (https://portal.gdc.cancer.gov/), PCa Data Base (PCaDB, http://bioinfo.jialab-ucr.org/PCaDB/), and cBioPortal (https://www.cbioportal.org/). The drug sensitive data were obtained from the Cancer Therapeutics Response Porta (CTRP)l[31] and CellMine[32]. Comparisons between immortalized Prostate Epithelial cells (PrEC-LH), Benign Prostatic Hyperplasia-1 cells (BPH-1), and the prostate adenocarcinoma

cell lines LNCaP and VCaP were conducted using the Cancer Dependency Map (DepMap) portal. The RNA-seq data for VCaP and R1AD1 PCa cell lines (upon DHT versus ENZ treatments) were based on the datasets GSE157107 and GSE135879, respectively. Transcriptomes of VCaP and LNCaP cells (upon siRNA-mediated AR knockdown) were derived from the datasets GSE82223. AR and H3K27ac chromatin binding profiles in VCaP cells were obtained from the datasets GSE55062 and GSE157105, respectively. Paired comparisons of individual PCa patients (before and after androgen deprivation therapy (ADT)) were based on the datasets GSE48403. AR and H3K27ac ChIP-Seq and ATAC-seq profiling of clinical PCa samples were sourced from the datasets GSE130408 and GSE70079. RNA-seq and AR ChIP-Seq in LN95 cells were from the datasets GSE171045 and GSE106559, respectively.

Bioinformatics analysis

The differentially expressed genes (DEGs) between PCa and normal control were identified utilizing the R package "limma"[33], with a cut-off criterion of |log2FoldChange|>2 and adjusted p-value < 0.05. The prognostic genes functionally associated with RNA-editing were identified through uni variate Cox regression analysis. The overlapping genes between DEGs and prognostic genes for relapse and overall survival were selected in the context of RNA-editing category. The R package "survminer" (https://github.com/kassambara/survminer) was employed to generate Kaplan-Meier (K-M) survival curves, and the R package "survivalROC"[34] was employed to plot receiver operating characteristic (ROC) curve and calculate the predictive power of RNA-editing genes.

The raw RNA-Seq reads were initially trimmed using TrimGalor (https://github.com/FelixKrueger/TrimGalore) with the following specific parameters: "-q 20 –phred33 –stringency 4 –length 20 -e 0.1". Subsequently, the clean reads were aligned to the hg19 human genome through STAR[35], configured with the parameters "–outSAMattributes NH HI NM MD –outSAMstrandField intronMotif –quantMode GeneCounts". For processing the ChIP-seq reads, trimming was conducted with Trim Galore under the same settings as for the RNA-seq. These trimmed reads were then mapped to the hg19 human genome using Bowtie2[36], with default parameters. The BAM files were processed through MACS2[37] for peak calling, with the parameters "–SPMR" and "–keep-dup = 1". Significant peaks were identified upon a q-value < 0.05. The resulted bedgraph files were converted into bigWig format using the UCSC bedGraphToBigWig tool. For multiple bigWig files, we would normalize the signals and then merged all cases within each group using the bigwigmerge tool[38]. These bigWig files were subsequently applied for track visualization with IGV[39].

Statistical analysis

The R platform version 4.4.1 (https://cran.r-project.org/) and GraphPad Prism 10.0 (GraphPad Software Inc, San Diego, CA, USA) were utilized to compute data and plot graphs. Our analyses were facilitated by various packages in the R platform. Group differences were assessed using ANOVA and Student's t-test, while for Kaplan-Meier survival analysis, the log-rank tests were used to calculate statistical significance in the clinical datasets. An adjusted p-value threshold of less than 0.05 was established to denote statistical significance across all tests.

Data availability

Data is provided within the manuscript and supplementary information files.

Received: 9 December 2024; Accepted: 25 April 2025
Published online: 22 May 2025

References

1. Massie, C. E. et al. The androgen receptor fuels prostate cancer by regulating central metabolism and biosynthesis. *EMBO J.* **30**, 2719–2733. https://doi.org/10.1038/emboj.2011.158 (2011).
2. Liang, J. et al. Androgen receptor splice variant 7 functions independently of the full length receptor in prostate cancer cells. *Cancer Lett.* **519**, 172–184. https://doi.org/10.1016/j.canlet.2021.07.013 (2021).
3. Robinson, D. et al. Integrative clinical genomics of advanced prostate cancer. *Cell* **161**, 1215–1228. https://doi.org/10.1016/j.cell.2015.05.001 (2015).
4. Antonarakis, E. S. et al. AR-V7 and resistance to enzalutamide and abiraterone in prostate cancer. *N Engl. J. Med.* **371**, 1028–1038. https://doi.org/10.1056/NEJMoa1315815 (2014).
5. Watson, P. A., Arora, V. K. & Sawyers, C. L. Emerging mechanisms of resistance to androgen receptor inhibitors in prostate cancer. *Nat. Rev. Cancer.* **15**, 701–711. https://doi.org/10.1038/nrc4016 (2015).
6. Scher, H. I. & Sawyers, C. L. Biology of progressive, castration-resistant prostate cancer: directed therapies targeting the androgen-receptor signaling axis. *J. Clin. Oncol.* **23**, 8253–8261. https://doi.org/10.1200/jco.2005.03.4777 (2005).
7. Baysal, B. E., Sharma, S., Hashemikhabir, S. & Janga, S. C. RNA editing in pathogenesis of Cancer. *Cancer Res.* **77**, 3733–3739. https://doi.org/10.1158/0008-5472.Can-17-0520 (2017).
8. Tassinari, V., Cesarini, V., Silvestris, D. A. & Gallo, A. The adaptive potential of RNA editing-mediated miRNA-retargeting in cancer. *Biochim. Biophys. Acta Gene Regul. Mech.* **1862**, 291–300. https://doi.org/10.1016/j.bbagrm.2018.12.007 (2019).
9. Qian, M., Spada, C. & Wang, X. Detection and application of RNA editing in Cancer. *Adv. Exp. Med. Biol.* **1068**, 159–170. https://doi.org/10.1007/978-981-13-0502-3_13 (2018).
10. Martinez, H. D. et al. RNA editing of androgen receptor gene transcripts in prostate cancer cells. *J. Biol. Chem.* **283**, 29938–29949. https://doi.org/10.1074/jbc.M800534200 (2008).
11. Salameh, A. et al. PRUNE2 is a human prostate cancer suppressor regulated by the intronic long noncoding RNA PCA3. *Proc. Natl. Acad. Sci. U S A.* **112**, 8403–8408. https://doi.org/10.1073/pnas.1507882112 (2015).
12. Han, L. et al. The genomic landscape and clinical relevance of A-to-I RNA editing in human cancers. *Cancer Cell.* **28**, 515–528. https://doi.org/10.1016/j.ccell.2015.08.013 (2015).
13. Liao, Y., Jung, S. H., Kim, T. & A-to-I RNA editing as a tuner of noncoding RNAs in cancer. *Cancer Lett.* **494**, 88–93. https://doi.org/10.1016/j.canlet.2020.08.004 (2020).
14. Ramírez-Moya, J. et al. An ADAR1-dependent RNA editing event in the cyclin-dependent kinase CDK13 promotes thyroid cancer hallmarks. *Mol. Cancer.* **20**, 115. https://doi.org/10.1186/s12943-021-01401-y (2021).

15. Shiromoto, Y., Sakurai, M., Minakuchi, M., Ariyoshi, K. & Nishikura, K. ADAR1 RNA editing enzyme regulates R-loop formation and genome stability at telomeres in cancer cells. *Nat. Commun.* **12**, 1654. https://doi.org/10.1038/s41467-021-21921-x (2021).
16. Jiang, L. et al. ADAR1-mediated RNA editing links ganglioside catabolism to glioblastoma stem cell maintenance. *J. Clin. Invest.* **132**. https://doi.org/10.1172/jci143397 (2022).
17. Siriwardena, S. U., Chen, K. & Bhagwat, A. S. Functions and malfunctions of mammalian DNA-Cytosine deaminases. *Chem. Rev.* **116**, 12688–12710. https://doi.org/10.1021/acs.chemrev.6b00296 (2016).
18. Swanton, C., McGranahan, N., Starrett, G. J. & Harris, R. S. APOBEC enzymes: mutagenic fuel for Cancer evolution and heterogeneity. *Cancer Discov.* **5**, 704–712. https://doi.org/10.1158/2159-8290.CD-15-0344 (2015).
19. Burns, M. B. et al. APOBEC3B is an enzymatic source of mutation in breast cancer. *Nature* **494**, 366–370. https://doi.org/10.1038/nature11881 (2013).
20. Ubhi, T. et al. Cytidine deaminases APOBEC3C and APOBEC3D promote DNA replication stress resistance in pancreatic cancer cells. *Nat. Cancer.* **5**, 895–915. https://doi.org/10.1038/s43018-024-00742-z (2024).
21. Christofi, T. & Zaravinos, A. RNA editing in the forefront of epitranscriptomics and human health. *J. Transl Med.* **17**, 319. https://doi.org/10.1186/s12967-019-2071-4 (2019).
22. Xu, Y., Chen, S. Y., Ross, K. N. & Balk, S. P. Androgens induce prostate cancer cell proliferation through mammalian target of Rapamycin activation and post-transcriptional increases in Cyclin D proteins. *Cancer Res.* **66**, 7783–7792. https://doi.org/10.1158/0008-5472.Can-05-4472 (2006).
23. Cai, C. et al. Androgen receptor gene expression in prostate cancer is directly suppressed by the androgen receptor through recruitment of lysine-specific demethylase 1. *Cancer Cell.* **20**, 457–471. https://doi.org/10.1016/j.ccr.2011.09.001 (2011).
24. Korenchuk, S. et al. VCaP, a cell-based model system of human prostate cancer. *Vivo* **15**, 163–168 (2001).
25. van Leenders, G. et al. The 2019 international society of urological pathology (ISUP) consensus conference on grading of prostatic carcinoma. *Am. J. Surg. Pathol.* **44**, e87–e99. https://doi.org/10.1097/pas.0000000000001497 (2020).
26. Amin, M. B. et al. The eighth edition AJCC Cancer staging manual: continuing to build a Bridge from a population-based to a more personalized approach to cancer staging. *CA Cancer J. Clin.* **67**, 93–99. https://doi.org/10.3322/caac.21388 (2017).
27. Yu, Z. et al. Rapid induction of androgen receptor splice variants by androgen deprivation in prostate cancer. *Clin. Cancer Res.* **20**, 1590–1600. https://doi.org/10.1158/1078-0432.Ccr-13-1863 (2014).
28. Mullard, A. RNA-editing drugs advance into clinical trials. *Nat. Rev. Drug Discov.* **23**, 323–326. https://doi.org/10.1038/d41573-024-00070-y (2024).
29. Booth, B. J. et al. RNA editing: expanding the potential of RNA therapeutics. *Mol. Ther.* **31**, 1533–1549. https://doi.org/10.1016/j.ymthe.2023.01.005 (2023).
30. Erion, D. M., Liu, L. Y., Brown, C. R., Rennard, S. & Farah, H. Editing Approaches to Treat Alpha-1 Antitrypsin Deficiency. *Chest* https://doi.org/10.1016/j.chest.2024.09.038 (2024).
31. Seashore-Ludlow, B. et al. Harnessing connectivity in a Large-Scale Small-Molecule sensitivity dataset. *Cancer Discov.* **5**, 1210–1223. https://doi.org/10.1158/2159-8290.Cd-15-0235 (2015).
32. Reinhold, W. C. et al. CellMiner: a web-based suite of genomic and Pharmacologic tools to explore transcript and drug patterns in the NCI-60 cell line set. *Cancer Res.* **72**, 3499–3511. https://doi.org/10.1158/0008-5472.Can-12-1370 (2012).
33. Ritchie, M. E. et al. Limma powers differential expression analyses for RNA-sequencing and microarray studies. *Nucleic Acids Res.* **43**, e47. https://doi.org/10.1093/nar/gkv007 (2015).
34. Heagerty, P. J., Lumley, T. & Pepe, M. S. Time-dependent ROC curves for censored survival data and a diagnostic marker. *Biometrics* **56**, 337–344. https://doi.org/10.1111/j.0006-341x.2000.00337.x (2000).
35. Dobin, A. et al. STAR: ultrafast universal RNA-seq aligner. *Bioinformatics* **29**, 15–21. https://doi.org/10.1093/bioinformatics/bts635 (2013).
36. Langmead, B. & Salzberg, S. L. Fast gapped-read alignment with bowtie 2. *Nat. Methods.* **9**, 357–359. https://doi.org/10.1038/nmeth.1923 (2012).
37. Zhang, Y. et al. Model-based analysis of ChIP-Seq (MACS). *Genome Biol.* **9**, R137. https://doi.org/10.1186/gb-2008-9-9-r137 (2008).
38. Guo, H. et al. Androgen receptor and MYC equilibration centralizes on developmental super-enhancer. *Nat. Commun.* **12**, 7308. https://doi.org/10.1038/s41467-021-27077-y (2021).
39. Robinson, J. T., Thorvaldsdottir, H., Turner, D. & Mesirov, J. P. igv.js: an embeddable javascript implementation of the integrative genomics viewer (IGV). *Bioinformatics* **39**. https://doi.org/10.1093/bioinformatics/btac830 (2022).

Acknowledgements

We would like to express our gratitude to Dr. Zhenyu Jia and Dr. Ruidong Li for making their PCaDB platforms available to us. Additionally, we are thankful for the TCGA, GEO, cBioPortal and other publicly accessible databases, along with the contributors who have shared their invaluable datasets.

Author contributions

Li-Yang Wang: Writing - Original Draft, Validation, Methodology, Visualization, Conceptualization and Funding acquisition. Ji Shi: Validation and Writing - review & editing. Mo-Fei Wang: Writing - review & editing. Yi-Meng Liu: Writing - review & editing. Hong-Shan Guo: Writing - review & editing. Jin-Cheng Wang: Writing - review & editing. Shu Jiang: Writing - review & editing. Jia-Qian Liang: Validation and Writing - review & editing. Xing-Hua Liao: Writing - review & editing and Funding acquisition. Shao-Yong Chen: Writing - review & editing, Supervision.

Funding

This work was supported by the Natural Science Basic Research Program of Shaanxi Province (#2023-JC-QN-0239), the National Department of Education Central Universities Research Fund (#GK202207004) and the University-Industry Collaborative Education Program (#231005940204433) to Li-Yang Wang and also funded by Wuhan Knowledge Innovation Project for Basic Research (#2022020801010523) to Jia-Qian Liang. This work was also financially supported by National Natural Science Foundation of China (#32170578); Hubei Natural Science Foundation (#2024AFB905 and #2022CFB026); Natural Science Foundation Exploration Program of Wuhan (#2024040801020310); the 14th Five Year Plan Hubei Provincial advantaged characteristics disciplines (groups) project of Wuhan University of Science and Technology (#2023C0303); Hubei Provincial Natural Science Foundation Huangshi Innovation and Development Joint Fund Project Cultivation Project (#2024AFD011); Huangshi Health Research Youth Talent Project (#WJ2024007); and Hubei Provincial Natural Science Foundation Huangshi Innovation and Development Key Project (#JCZRLH202501293) to Xing-Hua Liao.

Declarations

Competing interests
The authors declare no competing interests.

Additional information
Supplementary Information The online version contains supplementary material available at https://doi.org/10.1038/s41598-025-00169-1.

Correspondence and requests for materials should be addressed to J.-Q.L., X.-H.L. or S.-Y.C.

Reprints and permissions information is available at www.nature.com/reprints.

Publisher's note Springer Nature remains neutral with regard to jurisdictional claims in published maps and institutional affiliations.